

EVOLUTION OF CORONAL MASS EJECTION MORPHOLOGY WITH INCREASING HELIOCENTRIC DISTANCE. I. GEOMETRICAL ANALYSIS

N. P. SAVANI¹, M. J. OWENS^{2,3}, A. P. ROUILLARD^{4,5}, R. J. FORSYTH³, K. KUSANO^{1,6}, D. SHIOTA⁷, AND R. KATAOKA⁸

¹ Solar-Terrestrial Environment Laboratory, Nagoya University, Nagoya 464-8601, Japan; neel.savani02@imperial.ac.uk

² Space Environment Physic Group, University of Reading, Earley Gate, P.O. Box 243, Reading RG6 6BB, UK

³ The Blackett Laboratory, Imperial College London, Prince Consort Road London SW7 2BZ, UK

⁴ College of Science, George Mason University, Fairfax, VA 22030, USA

⁵ Space Science Division, Naval Research Laboratory, Washington, DC 20375, USA

⁶ Japan Agency for Marine-Earth Science and Technology, Yokohama, Kanagawa 236-0001, Japan

⁷ Computational Astrophysics Laboratory, Advanced Science Institute, RIKEN, 2-1, Hirosawa, Wako, Saitama 351-0198, Japan

⁸ Interactive Research Center of Science, Tokyo Institute of Technology, 2-12-1 Ookayama, Meguro, Tokyo 152-8551, Japan

Received 2010 December 15; accepted 2011 February 8; published 2011 March 30

ABSTRACT

At launch, coronal mass ejections (CMEs) are often approximated as locally cylindrical objects with circular cross sections. However, CMEs have long been known to propagate almost radially away from the Sun along with the bulk solar wind. This has important consequences for the structure of CMEs; an initially circular cross section will be severely flattened by this radial motion. Yet calculations of total flux and helicity transport by CMEs based on in situ observations still use the assumption of a locally cylindrical object. In this paper, we investigate the morphology of an interplanetary CME based upon geometric arguments. By radially propagating an initial cylindrical object that maintains a constant ratio between its expansion speed and bulk flow, A , we show that the flattening, or “pancaking,” of the two-dimensional cross section effectively ceases; the aspect ratios of these CMEs converge to a fixed value as they propagate further into the heliosphere. Thereafter the CME morphology is scale invariant. We predict aspect ratios of 5 ± 1 at terrestrial distances. By correlating a planetary shock with an interplanetary shock linked to a CME, these aspect ratios are estimated using in situ measurements in Paper II. These estimates are made at various heliocentric distances.

Key words: solar–terrestrial relations – solar wind – Sun: coronal mass ejections (CMEs)

Online-only material: color figures

1. INTRODUCTION

Coronal mass ejections (CMEs) drive the majority of the severe space weather events at Earth and affect the solar wind throughout the heliosphere (e.g., Howard & Tappin 2010). An improved understanding of the evolving morphology will provide better estimates for total helicity and improve calculations on the heliospheric flux budget (e.g., Owens & Crooker 2006). For these reasons, it is important to understand their spatial extent.

On the whole, the three-dimensional (3D) configuration of CMEs still remains unclear. As coronagraphs detect mostly photospheric light scattered off free electrons, they only provide a partial view of the CME structure which is projected onto the plane of the sky. However, the increased field of view and high sensitivity of the Large Angle and Spectrometric Coronagraph Experiment (LASCO) coronagraph has revealed much more structure within these events. In particular, circular striations have been observed in the cavities of three-part CMEs that suggest the presence of a helical or flux rope (FR) structure (Krall et al. 2001). Models for CMEs with morphology of an idealized FR have been successful in reproducing observations (e.g., Krall & St Cyr 2006; Rouillard et al. 2009a). These idealized FRs often possess circular cross sections (Chen et al. 1997; Thernisien et al. 2006) which are able to replicate the observed projections onto the plane of the sky. Work on the FR morphology also shows these objects often expand self-similarly (Chen 1996; Chen et al. 1997, 2000).

More recently, CMEs have been remotely observed beyond this region with the *STEREO* heliospheric imager (HI)

instrument (Kaiser et al. 2008; Eyles et al. 2009), and thereby increasing the coordinated effort between imaging and in situ observations (e.g., Mostl et al. 2009; Liu et al. 2010b; Rouillard et al. 2010a, 2010b). The different speeds of CMEs further into the heliosphere have been estimated by various methods (Mostl et al. 2009; Liu et al. 2010a) including the use of time-elongation analysis (Davies et al. 2009; Rouillard et al. 2009b; Williams et al. 2009; Davis et al. 2010); this method no longer includes the assumption of plane of sky propagation. Also, Savani et al. (2009) showed that the speed and power-law growth of the radial width of a single CME may now be monitored further into the heliosphere; the results were comparable to statistical surveys found from in situ analysis (Bothmer & Schwenn 1994, 1998). The extended fields of view of these instruments also allow tracking of CMEs out to the inner planets of our solar system (Davis et al. 2009; Rouillard et al. 2009a). From these observations, the evolution of the CME’s morphology has shown a stretching and flattening of the shape as it propagates radially away from the Sun.

As CMEs and the ambient solar wind propagate out into the heliosphere, they both travel essentially radially away for the Sun; this implies a significant deviation away from a self-similar expansion. But prior to the launch of *SMEI* and *STEREO*, there have been a limited number of remote heliospheric observations of CMEs. To bridge this gap in understanding the evolutionary changes to the CME morphology, numerical simulations of interplanetary CMEs (ICMEs) have been the primary tool to investigate the propagation of these transients. The realism and complexity of these heliospheric models have been continually improving and increasing (e.g., Riley

et al. 2001; Odstroil et al. 2004; Manchester et al. 2004; Kataoka et al. 2009; Nakamizo et al. 2009; Shiota et al. 2010). Now, fully 3D magnetohydrodynamic (MHD) simulations are regularly tested against observations. These simulations are not only compared to observations but are increasingly used to understand various properties that may affect the morphology, such as the deceleration processes of an ICME, interactions with the fast and slow ambient solar wind, and interactions of multiple ICMEs (e.g., Lugaz et al. 2005a). These simulations have shown that as FRs, initially with circular cross sections close to the Sun, propagate they evolve into flattened objects that are elliptical with a curved semimajor axis. This distorting due to expansion in spherical geometry has sometimes been referred to as “pancaking” (Riley & Crooker 2004). However, direct observational analysis to date is still primarily concerned with the non-radial cross section of the CME.

In this study, we analyze the morphology of CMEs using geometric arguments. We begin with previous estimates found by using single-point measurements using in situ data in Section 2. Later, in Section 3.1 we assume a constant rate of expansion and initial size to estimate the aspect ratio of CMEs as they propagate into the heliosphere. Section 3.2 then relaxes this assumption by allowing an expansion rate to vary with heliocentric distance. We discuss the consequences of this study in Section 4.

2. IN SITU ESTIMATES OF CME CROSS SECTION

In situ analysis of ICMEs provides a time series at a single point within the CME as it evolves and convects past the stationary spacecraft. This is often thought of as a 1D cut through a CME along the radial flow of the transient. The measured speeds and other properties of ICMEs, as measured in situ by spacecraft, often exhibit large event-to-event variability (e.g., Cane & Richardson 2003; Lepping et al. 2006, 2008). Therefore, a significant contribution in understanding the global orientation and morphology of ICMEs has come from investigations of FR models. A simple, yet successful, technique for modeling magnetic FRs in the solar wind and comparing them to measurements is the constant- α force-free model (Burlaga 1988; Lepping et al. 1990; Marubashi & Lepping 2007). From its first inception these models envisaged the ICMEs as cylindrical objects with circular cross sections, and whose magnetic field configuration can be described in terms of solutions to Bessel functions (Lundquist 1950).

However, surveys by Lepping and co-authors also showed many ICMEs have a linear decreasing velocity profile, indicative of an expanding CME. Therefore, more recent amendments to a static force-free model have been considered. Ad hoc modifications to the magnetic field vectors have been included to imitate CME expansions (Marubashi 1997). Later, Russell & Mulligan (2002b) relaxed the assumption of a circular cross section. This model often generates a better least-squares fit between the model and the data by increasing the number of free variables to the fit, but this does not necessarily prove that the model provides a more reliable reconstruction of the CME morphology. Owens et al. (2006) also tried to relax the circular cross-sectional assumption, but without increasing the number of free parameters which must be fit between model and observations. Starting with a force-free cylindrical structure close to the Sun, they propagated the FR radially away from the Sun. Owens et al. (2006) assumed the ratio between the radial expansion speed and the bulk flow to be a constant throughout the CME’s motion, resulting in an approximately elliptical cross

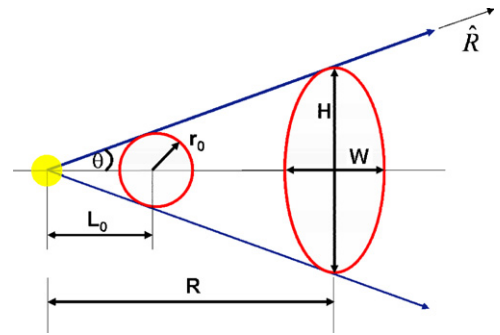


Figure 1. Schematic to display the geometry of a CME propagating into the heliosphere. The aspect ratio of the CME here represents the ratio between the vertical size, H , and width, W . The angular width, Ω , is equal to 2θ .

(A color version of this figure is available in the online journal.)

section in near-Earth space. Liu et al. (2006b) have also tried a kinematic approach to take steps toward solving the problem of understanding the full 3D shape of ICMEs.

3. GEOMETRICAL THEORY OF ICME SHAPE

In order to make estimates of the shape and size of CMEs we begin by studying initial conditions of an FR structure and observe how the cross section changes with heliospheric distance. The distortion from a circle to an ellipse may be quantified by a mathematical parameter called the aspect ratio; this is defined as the quotient of the semiminor axis to the semimajor axis. However, in this study the minor axis is the radial width of a CME, which we normalize to one, and then investigate the resulting length of the major axis. Therefore, this mathematical ratio is inverted in our study, so that the parameter is expected to be one or above. In Section 3.2, we investigate the aspect ratio if the expansion parameter is varied to fit statistical observations.

3.1. General Kinematic Framework

A CME can be regarded as a cylindrical magnetic FR at the beginning of its journey into the heliosphere. By kinematically evolving this structure, the vertical size of a CME can be predicted at any position in the heliosphere by assuming the plasma within the FR travels radially away from the Sun, as illustrated in Figure 1. In this example, the axis of the FR is perpendicular to the page and the solar rotation axis is pointing up. The cross section of an FR CME can be typically considered to begin with a radius of $r_0 \sim 1 R_s$ at an initial position of, $L_0 \sim 2 R_s$ away from the Sun center (Owens 2006; Owens et al. 2006). These values would produce a CME with an angular width of 53° , defined by

$$\Omega = 2\theta = 2 \arctan \left(\frac{r_0}{L_0} \right). \quad (1)$$

These approximate initial conditions have been validated with statistical estimation of CME widths using remote observations, resulting in a median width of $\sim 50^\circ$ (e.g., St Cyr et al. 2000; Cremades & Bothmer 2004; Cremades & St Cyr 2007). However, the uncertainty in this estimation increases with the angle between the plane of the sky and the direction of CME propagation. As illustrated in Figure 1, the vertical size (H) of a CME begins at $2r_0$, corresponding to the initial conditions of a cylindrical structure. Subsequently, the vertical size increases with increasing radial distance away from the Sun (R). The

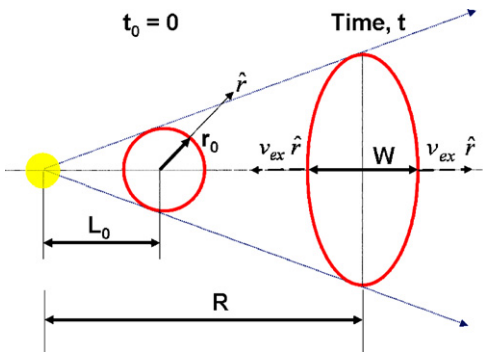


Figure 2. Schematic to display the geometry of a CME propagating into the heliosphere. The aspect ratio of a CME is shown to be affected by CME expansion.

(A color version of this figure is available in the online journal.)

vertical size as a function of heliocentric distance is therefore defined as

$$H = 2R \left(\frac{r_0}{L_0} \right). \quad (2)$$

In order to estimate the radial width (W) of a CME as a function of heliocentric distance, we must first estimate the expansion properties of a CME as it propagates. Figure 2 shows a schematic of the CME. The total width of a CME starts initially with the size of $2r_0$ and grows with time by $2V_{ex} \times t$. Here, t is defined as the time interval between its current state and the initial conditions and V_{ex} is the radial expansion velocity defined as the average velocity difference between the bulk flow and either the leading or the trailing edge.

The variable t can be converted to a function of heliocentric distance by re-arranging the simple velocity formula:

$$t = \frac{(R - L_0)}{V_{bulk}}. \quad (3)$$

Here, V_{bulk} is the bulk flow of the CME. By substituting Equation (3) to deduce the total width of the CME, we generate

$$W = 2r_0 + 2A(R - L_0), \quad (4)$$

where $A = V_{ex}/V_{bulk}$. It is important to point out here that the width and therefore the large-scale cross-sectional morphology of a CME are being affected not by the expansion rate alone, but by the ratio between the bulk flow and expansion.

As the CME propagates, the circular cross section deforms into an approximately ellipsoidal shape. The aspect ratio for CMEs, χ , therefore varies as a function of heliocentric distance, R , and the expansion ratio, A , and given by

$$\chi = \frac{R(r_0/L_0)}{r_0 + A(R - L_0)}. \quad (5)$$

Figure 3 shows the aspect ratio predicted by Equation (5) plotted as a function of heliocentric distance, in solar radii. The expansion ratio (A) is considered to be constant throughout the heliosphere. This assumption has previously been used for a kinematic treatment of CMEs as they propagate into the heliosphere (e.g., Owens et al. 2006; Owens 2008). This constant rate of expansion produces an interesting result; in that the aspect ratio is predicted to converge to a fixed value, suggesting the morphology of a CME remains approximately constant after reaching Venusian distances ($\sim 150 R_s$). This is contrary to the popular belief that, due to kinematic reasons, a CME continues to become more elongated as it evolves (e.g., Riley & Crooker 2004). An informal description for the changing morphology of such an ICME has been to call them ‘‘pancaking’’ in structure, but this analysis displays characteristics that the flattening for all intense and purposes ceases within the inner heliosphere. For this situation, the convergence of the aspect ratio follows a simple formula in the limit of $R \rightarrow \infty$:

$$\chi = \frac{r_0}{AL_0} = \frac{1}{A} \tan(\theta). \quad (6)$$

As the expansion ratio increases, the aspect ratio decreases to create an increasingly more circular cross section. In situ measurements at planetary distances have shown that the typical expansion ratio remains approximately constant with heliocentric distance and is of the order of ~ 0.1 (Owens et al. 2005; Forsyth et al. 2006 and references therein). This leads to a prediction

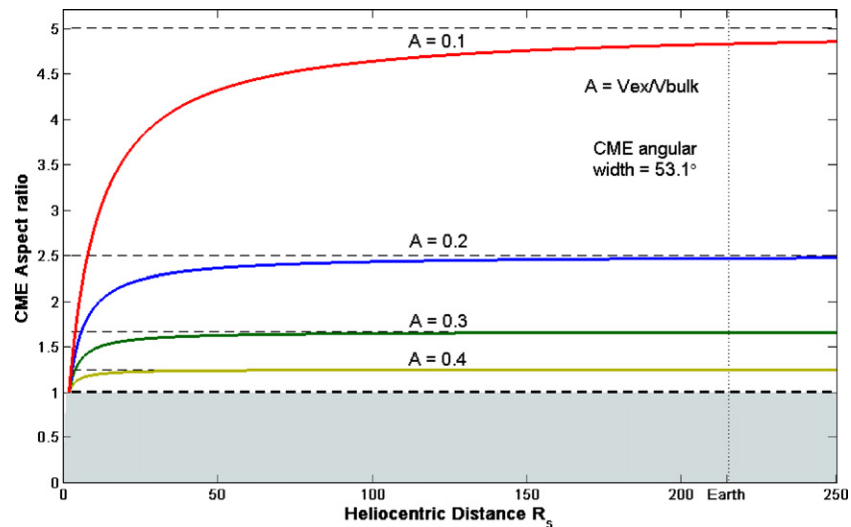


Figure 3. CME aspect ratio as a function of distance (solar radii). Different expansion ratios are displayed, with the more typical value of $A = 0.1$ shown in red. The results show converging values, producing a static morphology of an ICME. Aspect ratio of 1 represents a circular object while >1 indicates that the minor axis of an ellipse is along the radial line.

(A color version of this figure is available in the online journal.)

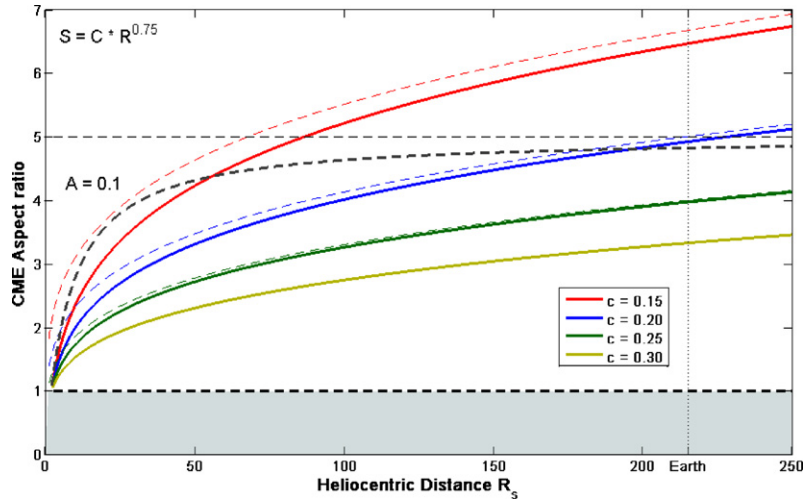


Figure 4. CME aspect ratio as a function of distance (solar radii). Different coefficients to the Bothmer & Schwenn (1998) method for CME expansion rate are displayed. Colored dashed and solid lines represent the substitution method and the expansion ratio method, respectively. The curved gray dashed line reproduces the curve shown in Figure 3 with $A = 0.1$.

(A color version of this figure is available in the online journal.)

that a CME aspect ratio between 4 and 6 would be expected throughout the heliosphere.

3.2. Vary the Expansion Velocity Ratio

The assumption of a constant expansion ratio is a limitation on the simple geometrical model we have implemented. In this section we relax that assumption. Instead of using a hypothetical growth term, we can include statistical work collected from in situ measurements onboard spacecraft. Previous in situ studies usually find the radius of a flux tube is expanding as a power law of distance R to the Sun, with an exponent close to unity (Bothmer & Schwenn 1994; Liu et al. 2004; Wang et al. 2005; Leitner et al. 2007). These studies have also been supported by a case study tracking a single CME into interplanetary space (Savani et al. 2009) and MHD models (e.g., Chen 1996).

For this study we will consider the empirical values defined by Bothmer & Schwenn (1998). This was based on a subset of ICMEs called magnetic clouds and included in situ data from many spacecraft over a wide range of heliocentric distances. The radial extent of each magnetic cloud, S , was measured by multiplying the average velocity measured with the time the spacecraft encountered the transient. For results obtained between the heliocentric distances of 0.3 and 4.2 AU, a linear regression was used to generate the empirical formula,

$$S(R) = C \times R^n, \quad (7)$$

where R is the heliocentric distance of the magnetic cloud, measured in AU, C and n are the empirically estimated coefficient and exponent values, respectively. There are two possible methods for using this equation to estimate the width of an ICME. Method 1, a direct substitution method, replaces the width (W) in Equation (4), with the new value of radial width, $S(R)$, which is then substituted into Equation (5). This is shown as the colored dashed curves displayed in Figure 4. This figure displays different solutions for a range of values of the coefficient, C , estimated as 0.24 ± 0.01 by Bothmer & Schwenn (1998). The dashed lines in Figure 5 show solutions obtained by varying the exponent, n , estimated as 0.78 ± 0.10 .

Method 2, a generalized expansion ratio method, deduces the width of a CME using Equation (7) indirectly. We use

the equation to create an expansion ratio that varies as a function of heliocentric distance. For this, we consider two arbitrary moments in time after the CME is initiated. At both of these moments we may predict the ICME radial width from Equation (7):

$$t_1 : S_1 = C \times R_1^n \quad t_2 : S_2 = C \times R_2^n. \quad (8)$$

During this time interval ($\Delta t = t_2 - t_1$), we are able to estimate the average bulk velocity and expansion speed as

$$V_{\text{bulk}} = \frac{(R_2 - R_1)}{\Delta t} \quad V_{\text{ex}} = \frac{\frac{1}{2}(S_2 - S_1)}{\Delta t}. \quad (9)$$

We are then able to convert the expansion ratio into a function of distance by eliminating the Δt :

$$A(R) = \frac{\frac{1}{2}(S(R) - S_1)}{(R - R_1)}. \quad (10)$$

Equation (10) shows that we can now vary the rate of expansion by specifying the coefficient and exponent in Equation (7) in the same way as the substitution method. Here, R_1 is the initial heliocentric distance (typically $2 R_s$); and R is the heliocentric distance of the CME, generalized from R_2 quoted in Equations (8) and (9). This new expansion rate as a function of heliocentric distance can then be implemented into the original aspect ratio formula in Equation (5). This expansion ratio method for removing the limitation imposed by a constant expansion ratio is represented by the solid curves in Figures 4 and 5.

Figure 4 shows how the aspect ratio varies for small variations of the coefficient term in Equation (7). The coefficient term is also the expected radial width of the CME at Earth; so the uncertainty of this term is related to the variability of CME size observed between many events. Any individual event at Earth could realistically arrive with a size between 0.2 and 0.25, but with an even more decreasing probability as the coefficient value moves away from this range. The large variability found in the widths and sizes of observed ICMEs is therefore expressed as an uncertainty in the aspect ratio in Figure 4. Figure 5 also

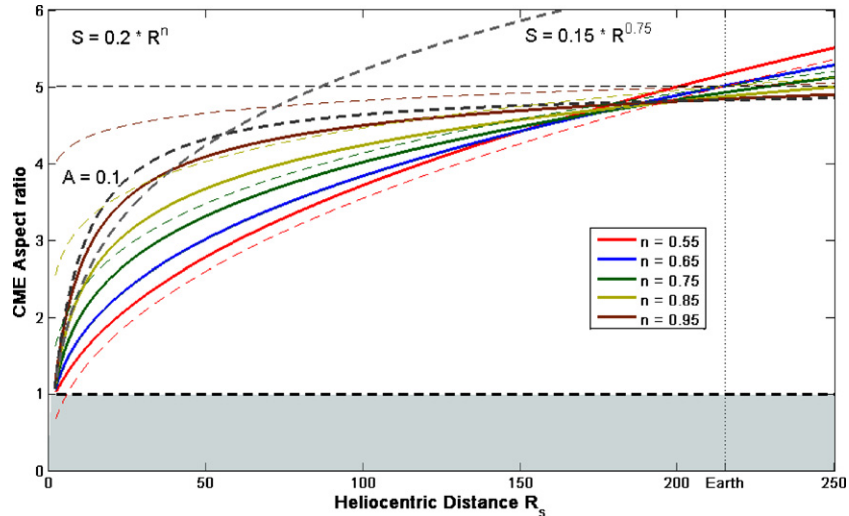


Figure 5. CME aspect ratio as a function of distance (solar radii). Different exponents to the Bothmer & Schwenn (1998) method for CME expansion rate are displayed. Colored dashed and solid lines represent the substitution method and the expansion ratio method, respectively. The curved gray dashed lines represent the curves shown in Figures 3 and 4.

(A color version of this figure is available in the online journal.)

highlights the possible deviation in aspect ratio if the exponent in Equation (7) was changed; this expresses the variability in growth rate of a CME as it propagates away from the Sun. In some part, this variable can be considered to express the average expansion ratio, A , parameter.

4. DISCUSSION AND CONCLUSIONS

This paper has investigated the aspect ratio, χ , of CMEs using geometrical arguments and found that they would be expected to $\sim 5 \pm 1$ at Earth. The evolution of the CME morphology has been assumed to continue to flatten as it travels further into the heliosphere, but in this paper we show that if the ratio between the expansion velocity and bulk flow remains constant then this aspect ratio converges to a fixed value, i.e., the CME morphology may become scale invariant as it propagates out into the heliosphere. Savani et al. (2010) observationally showed a case study event of a CME whose morphological changes appeared to occur predominately over a short range within the inner heliosphere using the inner HI camera onboard a *STEREO* spacecraft.

This is roughly consistent with observational estimates made from single spacecraft using in situ measurements (Russell & Mulligan 2002a; Liu et al. 2006b). However, a survey comparing the in situ data to the geometry is investigated further by Savani et al. (2011, herein referred to as Paper II); these authors display results that are less conclusive than previous estimates, in general the cross section is found to be more circular than would be suggested by geometric arguments.

Estimates using MHD simulations have qualitatively predicted the shape of ICMEs to flatten as they propagate into the heliosphere (Odstrcil & Pizzo 1999a; Riley & Crooker 2004; Lugaz et al. 2005b; Kataoka et al. 2009). Often colloquially termed as “pancaking,” it may be found useful to check the results of new MHD simulations for propagating CMEs with these geometrical estimates.

A blob of plasma within an ICME often expands in all directions in contrast to the solar wind which expands solely in the non-radial directions (as the solar wind has a nearly constant radial velocity for heliocentric distances ≥ 0.3 AU; Demoulin

et al. 2008). This implies the plasma density in an ICME decreases faster than the solar wind, explaining the low plasma density and pressures (Wang et al. 2005; Liu et al. 2006a). As the internal pressure driving the ICME expansion weakens, the expansion velocity becomes roughly constant (Wang et al. 2005), along with the bulk flow. If this ratio between expansion velocity and bulk flow does indeed become a constant, then the geometry of the aspect ratio dictates that the morphology of an ICME becomes scale invariant with heliocentric distance. However, as ICMEs propagate further into the heliosphere they often become embedded within merged interaction regions. Further work may consider if merged interaction regions (e.g., Rouillard et al. 2010c) are more likely to form before CMEs are able to relax into a scale-invariant structure.

The measured expansion velocity between events is highly variable, even for magnetic clouds traveling in “quiet” solar wind conditions (Demoulin et al. 2008). A small fraction of CMEs are found to be in compression, while about half are shown to have a velocity profile far from the idealized linear-with-time fit (Gulisano et al. 2010). The distorted velocity profile can be attributed to interaction with a fast solar wind stream or in some cases another CME. A theoretical analysis of the expansion velocity has been investigated by Gulisano et al. (2010). These authors re-characterized the expansion term by defining a non-dimensional factor. This factor displays a distribution much narrower than found with the expansion velocity and suggests a typical non-dimensional expansion rate. This term may provide further insight into the scale invariance, or otherwise, of the CME morphology.

As the expansion ratio decreases, the aspect ratio increases to create an increasingly more elliptical cross section. This has important consequences for determining the cross-sectional area and for the accuracy of estimates for the total flux content due to CMEs. As the radial component of the heliospheric magnetic field is found to be constant with latitude (Balogh et al. 1995; Smith & Balogh 1995), estimates of the total flux can be made in the near-Earth environment (Lockwood et al. 2004). Later, Owens & Crooker (2006) hypothesized that the total unsigned flux in the heliosphere may be contributed by two components; a constant background open flux and a time-varying component

from ICMEs. However, this study states that the estimated flux within an ICME is the most uncertain. This estimate was generated from an average of 132 magnetic clouds detected in situ and reliant on a constant- α force-free FR with a circular cross section (Lynch et al. 2005). As this paper has shown, these flux estimates would be heavily underestimated because of the enforced circular cross section. However, as hypothesized by Owens and Crooker, the estimates provided by Lynch et al. may in fact be overestimates due to a selection effect. Qualitatively, it may be possible that both of these opposing factors may be equal in strength and thereby minimize the uncertainty. At the very least, this paper shows that reasonable estimates for the aspect ratio, and therefore the cross-sectional area, can be made with just the angular width of the CME as stated in Equation (6).

Yamamoto et al. (2010) also suggest the poloidal flux considerations should be localized to part of the CME. By conserving the poloidal magnetic flux between magnetic clouds and their active regions, estimates of the axial length were made for regions where magnetic twists exist. This analysis also suggests that the evolution of CMEs is more localized, even though the magnetic fields may still be routed to the solar surface.

The assumption of a constant rate of expansion relative to the bulk flow may be considered as a simplification too far. In this paper, we have shown that if the expansion rate decreases with heliocentric distance, the aspect ratio would in fact increase. But by using in situ observations as the foundations of our estimates in the expansion rate we still find that after roughly 150 R_s the rate of change in the aspect ratio has decayed significantly, such that for terrestrial distances, a constant expansion rate may be assumed to a first approximation when estimating the cross-sectional area. By comparing the shape and structure of Earth's magnetosphere to an FR, Paper II will attempt to verify these aspect ratios with in situ observations.

Dynamic interaction of ambient solar wind changes this view dramatically. The time of launch with respect to the location of the slow and fast solar wind boundaries to the rear of the CME can have a significant effect on changing the cross-sectional shape of the CME (Odstreil & Pizzo 1999b). Simulations have shown that in fact the radial width of a given CME may differ by a factor of 2–3 at different locations as some parts are compressed and trapped by leading edge of the following fast stream.

N.P.S. thanks E. M. Henley, J. Mitchell, T. S. Horbury, and S. J. Schwartz of Imperial College London and V. Bothmer of University Göttingen, Germany for useful discussions.

REFERENCES

- Balogh, A., Smith, E. J., Tsurutani, B. T., Southwood, D. J., Forsyth, R. J., & Horbury, T. S. 1995, *Science*, 268:213, 1007
- Bothmer, V., & Schwenn, R. 1994, *Space Sci. Rev.*, 70:1, 215
- Bothmer, V., & Schwenn, R. 1998, *Ann. Geophys.*, 16:1, 1
- Burlaga, L. F. 1988, *J. Geophys. Res.*, 93, 7217
- Cane, H. V., & Richardson, I. G. 2003, *J. Geophys. Res.*, 108, 1156
- Chen, J. 1996, *J. Geophys. Res.*, 101, 27499
- Chen, J., et al. 1997, *ApJ*, 490:2, L191
- Chen, J., et al. 2000, *ApJ*, 533:1, 481
- Cremades, H., & Bothmer, V. 2004, *A&A*, 422:1, 307
- Cremades, H., & St Cyr, O. C. 2007, *Adv. Space Res.*, 40:7, 1042
- Davies, J. A., et al. 2009, *Geophys. Res. Lett.*, 36, L02102
- Davis, C. J., Davies, J. A., Lockwood, M., Rouillard, A. P., Eyles, C. J., & Harrison, R. A. 2009, *Geophys. Res. Lett.*, 36, L08102
- Davis, C. J., Kennedy, J., & Davies, J. A. 2010, *Sol. Phys.*, 263:1, 209
- Demoulin, P., Nakwacki, M. S., Dasso, S., & Mandrini, C. H. 2008, *Sol. Phys.*, 250:2, 347
- Eyles, C. J., et al. 2009, *Sol. Phys.*, 254:2, 387
- Forsyth, R. J., et al. 2006, *Space Sci. Rev.*, 123:1, 383
- Gulisano, A. M., Demoulin, P., Dasso, S., Ruiz, M. E., & Marsch, E. 2010, *A&A*, 509, A39
- Howard, T. A., & Tappin, S. J. 2010, *Space Weather*, 8, S07004
- Kaiser, M. L., Kucera, T. A., Davila, J. M., St Cyr, O. C., Guhathakurta, M., & Christian, E. 2008, *Space Sci. Rev.*, 136:1, 5
- Kataoka, R., Ebisuzaki, T., Kusano, K., Shiota, D., Inoue, S., Yamamoto, T. T., & Tokumaru, M. 2009, *J. Geophys. Res.*, 114, A10102
- Krall, J., Chen, J., Duffin, R. T., Howard, R. A., & Thompson, B. J. 2001, *ApJ*, 562:2, 1045
- Krall, J., & St Cyr, O. C. 2006, *ApJ*, 652:2, 1740
- Leitner, M., Farrugia, C. J., Mostl, C., Ogilvie, K. W., Galvin, A. B., Schwenn, R., & Biernat, H. K. 2007, *J. Geophys. Res.*, 112, A06113
- Lepping, R. P., Jones, J. A., & Burlaga, L. F. 1990, *J. Geophys. Res.*, 95A8, 11957
- Lepping, R. P., Wu, C. C., Berdichevsky, D. B., & Ferguson, T. 2008, *Ann. Geophys.*, 26:7, 1919
- Lepping, R. P., et al. 2006, *Ann. Geophys.*, 24:1, 215
- Liu, Y., Davies, J. A., Luhmann, J. G., Vourlidas, A., Bale, S. D., & Lin, R. P. 2010a, *ApJ*, 710:1, L82
- Liu, Y., Richardson, J. D., & Belcher, J. W. 2004, *Planet Space Sci.*, 53, 3
- Liu, Y., Richardson, J. D., Belcher, J. W., & Kasper, J. C. 2006a, *J. Geophys. Res.*, 111, A01102
- Liu, Y., Richardson, J. D., Belcher, J. W., Wang, C., Hu, Q., & Kasper, J. C. 2006b, *J. Geophys. Res.*, 111, A12S03
- Liu, Y., Thernisien, A., Luhmann, J. G., Vourlidas, A., Davies, J. A., Lin, R. P., & Bale, S. D. 2010b, *ApJ*, 722:2, 1762
- Lockwood, M., Forsyth, R. J., Balogh, A., & McComas, D. J. 2004, *Ann. Geophys.*, 22:4, 1395
- Lugaz, N., Manchester, W. B., & Gombosi, T. I. 2005a, *ApJ*, 634:1, 651
- Lugaz, N., Manchester, W. B., & Gombosi, T. I. 2005b, *ApJ*, 627:2, 1019
- Lundquist, S. 1950, *Ark. Fys.*, 24, 361
- Lynch, B. J., Griesbeck, J. R., Zurbuchen, T. H., & Antiochos, S. K. 2005, *J. Geophys. Res.*, 110, A08107
- Manchester, W. B., et al. 2004, *J. Geophys. Res.*, 109, A01102
- Marubashi, K. 1997, in *Coronal Mass Ejections*, ed. N. U. Crooker, J. A. Joselyn, & J. Feynman (Geophys. Monogr. 99; Washington, DC: AGU), 147
- Marubashi, K., & Lepping, R. P. 2007, *Ann. Geophys.*, 25:11, 2453
- Mostl, C., et al. 2009, *ApJ*, 705:2, L180
- Nakamizo, A., Tanaka, T., Kubo, Y., Kamei, S., Shimazu, H., & Shinagawa, H. 2009, *J. Geophys. Res.*, 114, A07109
- Odstreil, D., & Pizzo, V. J. 1999a, *J. Geophys. Res.*, 104, 483
- Odstreil, D., & Pizzo, V. J. 1999b, *J. Geophys. Res.*, 104, 493
- Odstreil, D., Riley, P., & Zhao, X. P. 2004, *J. Geophys. Res.*, 109, A02116
- Owens, M. J. 2006, *J. Geophys. Res.*, 111, A12109
- Owens, M. J. 2008, *J. Geophys. Res.*, 113, A12102
- Owens, M. J., Cargill, P. J., Pagel, C., Siscoe, G. L., & Crooker, N. U. 2005, *J. Geophys. Res.*, 110, A01105
- Owens, M. J., & Crooker, N. U. 2006, *J. Geophys. Res.*, 111, A10104
- Owens, M. J., Merkin, V. G., & Riley, P. 2006, *J. Geophys. Res.*, 111, A03104
- Riley, P., & Crooker, N. U. 2004, *ApJ*, 600:2, 1035
- Riley, P., Linker, J. A., & Mikic, Z. 2001, *J. Geophys. Res.*, 106, 15889
- Rouillard, A. P., et al. 2009a, *J. Geophys. Res.*, 114, A07106
- Rouillard, A. P., et al. 2009b, *Sol. Phys.*, 256:1, 307
- Rouillard, A. P., et al. 2010a, *J. Geophys. Res.*, 115, A04103
- Rouillard, A. P., et al. 2010b, *J. Geophys. Res.*, 115, A04104
- Rouillard, A. P., et al. 2010c, *ApJ*, 719:2, 1385
- Russell, C. T., & Mulligan, T. 2002a, *Planet. Space Sci.*, 50:5, 527
- Russell, C. T., & Mulligan, T. 2002b, *Adv. Space Res.*, 3, 301
- Savani, N. P., Owens, M. J., Rouillard, A. P., Forsyth, R. J., & Davies, J. A. 2010, *ApJ*, 714:1, L128
- Savani, N. P., Rouillard, A. P., Davies, J. A., Owens, M. J., Forsyth, R. J., Davis, C. J., & Harrison, R. A. 2009, *Ann. Geophys.*, 27:11, 4349
- Savani, N. P., et al. 2011, *ApJ*, in press
- Shiota, D., Kusano, K., Miyoshi, T., & Shibata, K. 2010, *ApJ*, 718:2, 1305
- Smith, E. J., & Balogh, A. 1995, *Geophys. Res. Lett.*, 22:23, 3317
- St Cyr, O. C., et al. 2000, *J. Geophys. Res.*, 105, 18169
- Thernisien, A. F. R., Howard, R. A., & Vourlidas, A. 2006, *ApJ*, 652:1, 763
- Wang, C., Du, D., & Richardson, J. D. 2005, *J. Geophys. Res.*, 110, A10107
- Williams, A. O., Davies, J. A., Milan, S. E., Rouillard, A. P., Davis, C. J., Perry, C. H., & Harrison, R. A. 2009, *Ann. Geophys.*, 27:12, 4359
- Yamamoto, T. T., Kataoka, R., & Inoue, S. 2010, *ApJ*, 710:1, 456